ELSEVIER

Inorganica Chimica Acta 229 (1995) 195–202

Inorganica Chimica Acta

Transition metal complexes of a tridentate biquinone ligand: electronic structures, charge distributions and magnetic properties ☆

Tong Ren

Department of Chemistry, Florida Institute of Technology, Melbourne, FL 32901, USA

Received 7 June 1994

Abstract

The electronic structures of the neutral transition metal (M) complexes *mer*-M(HDBQI)$_2$, where HDBQI is 3,5-di-tert-butyl-1,2-quinone 1-(2-hydroxy-3,5-di-tert-butylphenyl)imine, with M = Ti, V, Mn, Ni and Co have been explored with Fenske–Hall molecular orbital calculations. It has been demonstrated that the frontier orbitals of these complexes are, in general, determined by the differences in energy between the d orbitals of the metal center and the π acceptor orbitals of HDBQI, especially the $5b_2$ orbital. Most of the theoretical assignments of the formal oxidation states, i.e. Ti as 4+, Mn as 4+, Co as 3+ and Ni as 2+, are consistent with those determined experimentally. The only exception is V, which should be 5+, instead of the previously assumed 4+. This finding has been discussed in conjunction with the spectroscopic features of the V complex. The previously proposed superexchange ferromagnetic coupling mechanism for the Ti complex is strongly supported by the observation that the d_π orbitals of Ti contribute significantly to the organic radical orbitals.

Keywords: Electronic structure; Magnetism; Transition metal complexes; Polydentate ligand complexes; Biquinone complexes

1. Introduction

There has been considerable interest in the coordination chemistry of 3,5-di-tert-butyl-1,2-quinone 1-(2-hydroxy-3,5-di-tert-butylphenyl)imine (HDBQI) [1] in recent years. The structural, spectroscopic, electrochemical and magnetic properties of *mer*-M(HDBQI)$_2$ complexes, which are readily prepared from the aerobic Schiff-base condensation of 3,5-di-tert-butyl-1,2-benzoquinone with M as the template, have been extensively explored. In the early work of Girgis and Balch [1], the syntheses and some spectroscopic features of the complexes with M = Mg, Fe, Ni, Cu, Zn and Cd were reported. Pierpont and co-workers extended this chemistry to Co and Mn and also provided X-ray structures, spectroscopic features and voltammetries of the complexes with M = Ni, Co, Fe and Mn [2,3]. The variety of this chemistry was further demonstrated by the recent work of Dei and co-workers, where the complexes with M = Ti, V, Sn and Ge were investigated [4,5].

The most striking feature of HDBQI as a ligand is that it can formally adopt a +1 (BQ–N–BQ), 0 (SQ–N–BQ), −1 (Cat–N–BQ), −2 (Cat–N–SQ) or −3 (Cat–N–Cat) charge, as depicted in Scheme 1 (modified according to Pierpont [3], the 3,5-tert-Bu groups were omitted for the sake of clarity). The formal oxidation state that the ligand adopts in the complex is determined by the nature of the metal center. The charge distribution between the metal center and the ligands has been the focus of most research in this area. On the basis of structural and magnetic characteristics, the complexes of Ti, V, Mn, Ge and Sn were formally designated as

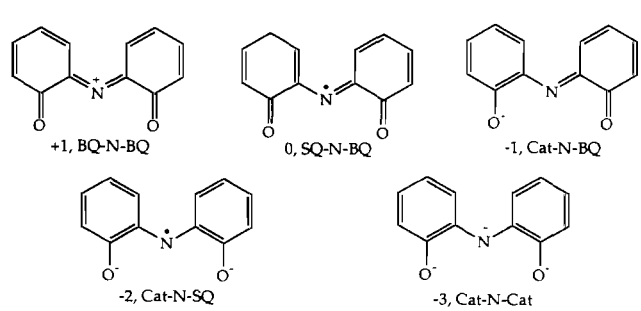

Scheme 1.

☆ This paper is dedicated to my mentor Professor F. Albert Cotton on the occasion of his 65th birthday.

SSDI 0020-1693(94)04245-Q

$M^{IV}(Cat\text{–}N\text{–}SQ)_2$, those of Fe and Co as $M^{III}(Cat\text{–}N\text{–}SQ)(Cat\text{–}N\text{–}BQ)$, and those of Ni, Cu and Zn as $M^{II}(Cat\text{–}N\text{–}BQ)_2$ [3,5].

We took notice that while such an assignment is unambiguous for main group metal complexes, it is not the case for the transition metal complexes due to the proximity in energies of the metal d orbitals to the ligand acceptor orbitals. Although geometric parameters such as M–O and M–N distances are normally very sensitive to the oxidation state of the metal center, they are less revealing when a redox non-innocent ligand is involved. While magnetic susceptibility and magnetic resonance spectroscopy are powerful tools in determining the electron configuration of the metal center, they are not sufficient here since HDBQI is a radical in two possible oxidation states. Therefore molecular orbital calculations with reasonable accuracy become a complementary tool to the experimental methods in the determination of the charge distribution in these complexes.

The phenyl ring is an indispensable functional group in the description of the electronic properties of any quinoid ligand. However, the inclusion of four phenyl rings renders the computation at high level of accuracy (ab initio) a formidable task. Therefore the Fenske–Hall method [6] has been chosen for its reliability and efficiency in handling large transition metal complexes and clusters. It is also encouraging to note that the Fenske–Hall method has been successful in reproducing the charge distributions derived from the EPR experiment for the catecholate complexes of Cr and V [7]. In this paper, the MO analysis for the structurally characterized 3d metal complexes with M as Ti, V, Mn, Co and Ni are presented. General patterns of the bonding interactions between the d orbitals of the M and the high energy ligand π orbitals are analyzed in detail. Based on this analysis the charge distribution in each complex is assigned and discussed. Furthermore, the identities of the observed multistep one-electron redox processes for these complexes are analyzed within the single-electron MO schemes. Finally, the mechanism for the ferromagnetic couplings observed for the Ti complexes is addressed.

2. Computational procedures

Fenske–Hall molecular orbital calculations [6] were performed on a VAX station 4000 VLC. Basis functions used were generated by the numerical Xα atomic orbital program [8] in conjunction with an Xα-to-Slater basis program [9,10].

Geometric parameters of the free ligand of -2 charge were derived from those determined for Cat–N–SQ in the $Ti(Cat\text{–}N\text{–}SQ)_2$ structure [5], and the geometry of the ligand was idealized to C_{2v} symmetry. The molecular plane was coincident with the XZ plane. Geometrical parameters of $M(HDBQI)_2$ were adapted from the tabulation of Simpson et al. [3] for M = Mn, Ni and Co, and that of Bruni et al. [5] for M = Ti and V. The C–H distance was set to 1.05 Å. All the complexes were idealized to D_{2d} point symmetry, with one ligand (L1) placed in the upper half of the XZ plane, and the other (L2) placed in the lower half of the YZ plane. With the XY plane being rotated by $\pi/4$ from the conventional D_{2d} setting [11], the basis functions for b_1 and b_2 became xy and x^2-y^2, respectively. The only simplification in the structure of the model complex is the replacement of both 3- and 5-tert-butyl groups of HDBQI with hydrogen atoms.

3. Results

3.1. Free ligand

There are 38 occupied valence orbitals for Cat–N–SQ, 15 are of the symmetry a_1, 4 of a_2, 14 of b_1 and 5 of b_2. The HOMO is a singly occupied $5b_2$ and the LUMO is $6a_2$. Most of the low energy valence orbitals are of C–C, C–N, C–O and C–H σ bonding and C–C π bonding characters, and these are omitted from the discussion. However, the characteristics of the six occupied orbitals of the highest energies are particularly interesting due to their capability to strongly interact with the metal valence orbitals. These orbitals can be classified into two groups: σ donor orbitals and π donor/acceptor orbitals. The orbitals $14b_1$, $15a_1$ and $14a_1$ are predominantly sp^2 lone pairs localized on oxygen (87%), oxygen (90%) and nitrogen (75%), respectively. These orbitals are oriented toward the metal center and are the major constituents of both M–O and M–N σ bonds in the complex. In the second group, $5b_2$ and $4b_2$ are mainly the π orbitals localized over the O(1)–N–O(2) linkage (which accounts for $\sim$40% in charge distribution in both cases) and the phenyl rings as well, while $4a_2$ is a π orbital localized on two oxygen sites (67%) with some extension to the phenyl rings. These high energy π orbitals and their combinations will contribute to most of the M–L π interactions, keys to determining the nature of the frontier orbitals. Qualitative pictures of these orbitals are sketched in Fig. 1. As shown in this Figure, the HOMO is essentially an antibonding π orbital along the O(1)–N–O(2) linkage. A π antibonding orbital localized on the phenyl rings, the LUMO $6a_2$ is of much higher energy (7.5 eV above the HOMO). The interaction of the LUMO with metal orbitals is very unlikely due to both the mismatch in energy and the absence of appropriate orbital overlap.

Since the HOMO of the free Cat–N–SQ is the half-filled $5b_2$, it is possible to add an additional electron to this orbital, which yields Cat–N–Cat (3−). Due to

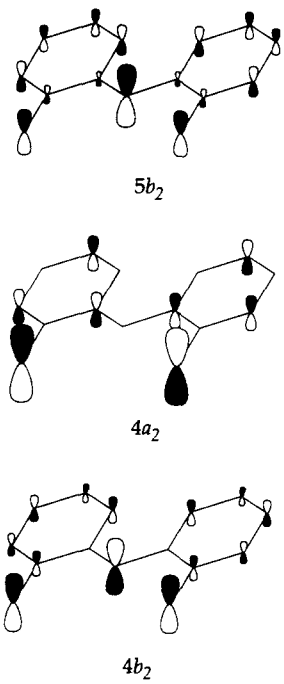

Fig. 1. Qualitative representations of the high energy π orbitals of HDBQI. The symmetry labels are for C_{2v} point symmetry.

the antibonding nature of $5b_2$, this addition of an electron eliminates the π conjugation between the two quinoid units, which is energetically unfavorable unless the metal center is extremely reducing. In contrast, one electron can be removed from $5b_2$ to give a monoanion Cat–N–BQ when the metal center is not strongly reducing in nature. Complete removal of the antibonding electrons from $5b_2$ should 'restore' one π bond, and thus the empirical resonance structure of Cat–N–BQ shown in Scheme 1 is substantiated. Due to the limitations of Fenske–Hall methodology, it is not realistic to extend such a discussion to the more oxidized forms, i.e. SQ–N–BQ and BQ–N–BQ, on the basis of a single electron calculation of Cat–N–SQ.

3.2. Symmetry properties of $M(HDBQI)_2$

Since all the complexes under consideration adopt similar pseudooctahedral geometries with the same D_{2d} symmetry, it is worthwhile carrying out a symmetry analysis of the possible M–L interactions based on the results for the free ligand. Among the valence orbitals available for a 3d metal ion, the conventional d^2sp^3 hybrid orbitals will comprise six σ-type metal acceptor orbitals, i.e. 4s (a_1), $4p_{x,y,z}$ ($e+b_2$), d_{z^2} (a_1) and $d_{x^2-y^2}$ (b_2). The symmetry combinations among the σ donor orbitals (three from each of the two ligands) are as follows: $2a_1+2a_1'$ (C_{2v}) $=2a_1+2b_2$ (D_{2d}) and b_1+b_1' (C_{2v}) $=e$ (D_{2d}). The normal C_{2v} Mulliken symbols are used for the ligand orbitals from L1, and the primed Mulliken symbols for those from L2 (see Section 2). The traditional e_g^* set (d_{z^2} and $d_{x^2-y^2}$), strongly repelled by the σ antibonding interactions, is of high energy and unfilled in most cases. Unless a Jahn–Teller axial elongation exists, d_{z^2} is of higher energy than $d_{x^2-y^2}$ since N is a better σ donor. In D_{2d} symmetry three d_π orbitals (the conventional t_{2g} set) are divided into two sets: d_{xy} (b_1) and $d_{xz,yz}$ (e). There is only one π type ligand orbital available to interact with the former, i.e. a b_1 symmetry combination of the p_π orbitals localized on the oxygen atoms (C_{2v}: a_2+a_2'), as depicted in Fig. 2(a). However, there are a variety of e type ligand orbitals with the potential to overlap with $d_{xz,yz}$ orbitals. The three major contributors to the d_{xz} orbital are drawn in Fig. 2(b): the strongest overlap comes from the p_x orbital localized on the N atom of L2; the sp^2 hybrid lone pair orbitals on the oxygen atoms of L1 (the other sp^2 hybrids are involved in both C–O and O–M σ bonding) also have significant overlap. The p_x orbital of the N atom of L1 has the smallest contribution of the three, since it is primarily involved in N–C σ bonds. Since the d_{xy} orbital has better overlap with the π-donor orbital ($4a_2$ (C_{2v}) in the free ligand is always filled), it will be of higher energy than $d_{xz,yz}$. Therefore, the ligand field splitting pattern is expected as follows: $d_{xz,yz} < d_{xy} \ll d_{x^2-y^2} < d_{z^2}$.

For the model complexes under consideration, there are up to 79 occupied valence molecular orbitals contributed from the combinations of the 76 (2×38) occupied MOs of the ligand and the valence orbitals of the metal center. Among these orbitals, 15 are of a_1

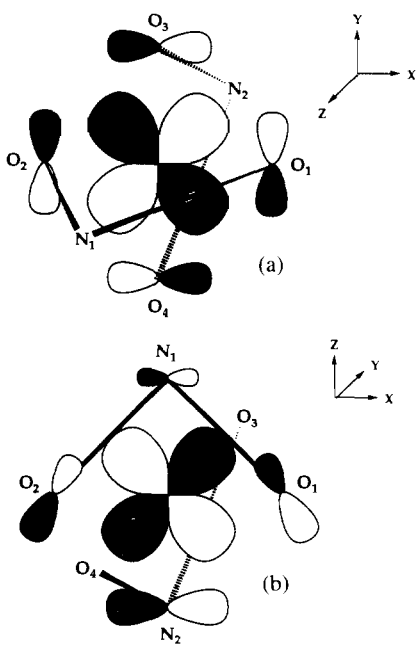

Fig. 2. Patterns of π orbital interactions between the metal center and the ligands. Phenyl rings are omitted and the linkage between N–O is symbolized by a bold line. (a) b_1 type; (b) e type, x-component is drawn.

symmetry, 4 of a_2, 5 of b_1, 15 of b_2 and 20 of e. Most correspond to either the C–C, C–H, C–O and C–N σ bonds or the low energy C–C, C–O and C–N π bonds, and are of less interest to the current discussion. For all five model complexes, the symmetries, energies, and characters of selected upper energy valence orbitals from Fenske–Hall calculations are given in Table 1. For more detailed tabulations, see Section 6.

3.3. $Ti(L)_2$

There are 76 occupied valence molecular orbitals for the complex. Of the frontier orbitals, the HOMO (19e) consists of a pair of singly occupied ligand-based π orbitals with dominant contribution from N (24%) and each of its two components contains the contribution from one of the ligands only. Therefore the HOMO orbitals are mutually orthogonal, and each represents an organic radical localized on one ligand. It is also worthwhile mentioning that there is a significant, albeit small, contribution from the $d_{xz,yz}$ orbitals (7%) to the HOMO. The LUMO 20e, 6.7 eV above the HOMO, are essentially the metal centered $d_{xz,yz}$ orbitals (78%) with a minor contribution from the ligand orbitals. The next unoccupied molecular orbital, $5b_1$, is also a metal centered orbital (d_{xy}, 67%). The e_g* set, which is roughly 12 eV above the t_{2g} set, is separated into $16b_2$ ($d_{x^2-y^2}$) and $16a_1$ (d_{z^2}). The d_{z^2} is below the $d_{x^2-y^2}$ because the Ti–N bond is significantly longer than the Ti–O bond. The orbitals listed beneath the HOMO are all ligand-based with the Ti contributing no more than 10%.

3.4. $V(L)_2$

In comparison with $Ti(L)_2$, the vanadium complex has one additional valence electron, which should occupy the 19e orbital, the half-filled HOMO of the Ti complex. The calculation indeed indicates that the 19e is the triply occupied HOMO among the 76 occupied valence orbitals. Since the HOMO is a ligand π orbital, there is only one organic radical in the complex. The metal-centered $d_{xz,yz}$ orbitals are the LUMO (20e) which is 4.83 eV above the HOMO. The next virtual orbital $5b_1$ is the metal centered d_{xy} orbital. The overall features of the calculation with V, and especially the compositions of the frontier orbitals, are very similar to those of Ti. A subtle, nevertheless important, difference is that the d orbital contributions to the occupied MOs in the V complex are more pronounced, as demonstrated by the fact that there is 17% $d_{xz,yz}$ character in the HOMO versus the 7% in that of the Ti complex.

3.5. $Mn(L)_2$

There are 77 occupied valence molecular orbitals for this complex. For the frontier orbitals, the singly occupied $5b_1$ (d_{xy}, 61%) is the HOMO, a pair of ligand-dominant π-antibonding (also 38% $d_{xz,yz}$) orbitals (20e) is the LUMO, and the HOMO–LUMO gap is about 0.68 eV. The MO pattern for the Mn complex is distinguished from those for both the Ti and V complexes by the high degree of mixing between the t_{2g} orbitals and the ligand π orbitals: orbitals 19e and 17e contain 35% and 22% $d_{xz,yz}$ characters, respectively, and orbital $4b_1$ contains 23% d_{xy} character.

3.6. $Co(L)_2$

The addition of two valence electrons (compared with the Mn case) increases the number of occupied valence orbitals to 78. The HOMO 20e consists of a pair of ligand based π orbitals with an occupancy of one. The $d_{x^2-y^2}$ is the LUMO ($16b_2$), which is 6.6 eV above the HOMO. The occupied valence orbitals with dominant or large d_π contributions are, in descending order of energy: $5b_1$ (d_{xy}, 49%), 19e ($d_{xz,yz}$, 46%), $4b_1$ (d_{xy}, 43%) and 18e ($d_{xz,yz}$, 35%). The t_{2g} set orbitals are fully occupied. The e_g* set is empty, yet it is energetically much closer to the occupied orbitals in comparison with all of the previous complexes.

3.7. $Ni(L)_2$

The HOMO (20e) is comprised of a pair of singly occupied ligand based π orbitals with a minimal contribution from $d_{xz,yz}$ (2%). The LUMO ($16b_2$), which is 0.41 eV above the HOMO, is the antibonding orbital of the Ni–O σ bond with a 37% contribution from $d_{x^2-y^2}$. The next virtual orbital, $16a_1$, is the antibonding orbital of the Ni–N σ bond with 40% character from the d_{z^2} orbital. Three low lying ($\sim$8 eV below the HOMO) molecular orbitals can be unambiguously attributed to the t_{2g} set: $3b_1$ as d_{xy} (57%) and 17e as $d_{xz,yz}$ (62%). Other π orbitals with significant d_π characters are 16e (12% $d_{xz,yz}$) and $2b_1$ (28% d_{xy}). As a result of the extensive mixing between the d orbitals and the ligand orbitals, the covalency of M–L σ bonds has been dramatically increased: there is 23% $d_{x^2-y^2}$ character in $14b_2$ and 22% d_{z^2} in $14a_1$.

These results clearly demonstrate that the position of the transition element in the Periodic Table determines the nature of M–L π interactions. For the early transition elements Ti and V, the d_π orbitals (free ion) are far above the ligand π orbitals (free ligand, C_{2v}: $5b_2$ and $4a_2$). Therefore, the ligand π orbitals dominate the bonding/non-bonding molecular orbitals (D_{2d}: 19e, 18e, $4a_2$ and $4b_1$), while the d_π orbitals dominate the antibonding counterparts (D_{2d}: 20e and $5b_1$), and the two groups are separated by a significant HOMO–LUMO gap. For the middle transition element Mn, the d_π orbitals are only slightly above the π(L)s in energy. As a result, extensive mixing exists between

Table 1
Upper valence molecular orbitals of $M(HDBQI)_2$ [a]

Ti(Cat–N–SQ)^2			V(Cat–N–SQ)(Cat–N–Cat)			Mn(Cat–N–SQ)$_2$			Co(Cat–N–SQ)(Cat–N–BQ)			Ni(Cat–N–BQ)$_2$		
MO	E (eV)	Character [b]	MO	E (eV)	Character [b]	MO	E (eV)	Character [b]	MO	E (eV)	Character [b]	MO	E (eV)	Character [b]
$16b_2$	12.03	d_{x2-y2}	$16a_1$	9.83	d_{z2}									
$16a_1$	10.87	d_{z2}	$16b_2$	9.53	d_{x2-y2}	$16a_1$	6.01	d_{z2}						
$5b_1$	−1.48	d_{xy}	$5b_1$	−4.35	d_{xy}	$16b_2$	3.67	d_{x2-y2}	$16a_1$	1.74	d_{z2}	$16a_1$	−5.79	d_{z2}
20e	−2.14	LUMO, $d_{xz,yz}$	20e	−4.65	LUMO, $d_{xz,yz}$	20e	−6.73	LUMO, $d_{xz,yz}$	$16b_2$	−0.95	LUMO, d_{x2-y2}	$16b_2$	−7.53	LUMO, d_{x2-y2}
19e	−8.86	HOMO, $2e^-$ π(L)	19e	−9.48	HOMO, $3e^-$ π(L)	$5b_1$	−7.41	HOMO, $1e^-$ d_{xy}	20e	−7.57	HOMO, $1e^-$ π(L)	20e	−7.94	HOMO, $2e^-$ π(L)
$4a_2$	−11.05	π (L)	$4a_2$	−11.40	π (L)	19e	−10.01	$d_{xz,yz}$ & π(L)	$5b_1$	−9.39	d_{xy} & π(L)	$5b_1$	−10.93	π (L)
18e	−12.43	π (L)	18e	−12.83	π (L)	$4a_2$	−11.00	π (L)	$4a_2$	−10.86	π (L)	$4a_2$	−11.03	π (L)
$4b_1$	−12.63	π (L)	$4b_1$	−13.24	π (L)	18e	−12.63	π (L)	19e	−11.14	$d_{xz,yz}$	19e	−12.12	π (L)
17e	−12.82	π (L)	$15b_2$	−13.64	σ (N–M)	$4b_1$	−12.97	π (L)	18e	−12.48	π (L)	18e	−12.77	π (phen)
$15b_2$	−12.97	σ (L–M)	17e	−13.69	π (L)	$15a_1$	−13.46	σ (L–M)	$4b_1$	−13.25	d_{xy} & π(L)	$15b_2$	−13.56	σ (L–M)
$15a_1$	−13.24	σ (L–M)	$15a_1$	−13.84	σ (O–M)	17e	−13.59	π (L)	$15a_1$	−13.42	σ (L–M)	$15a_1$	−13.68	σ (L–M)
						$15b_2$	−13.66	σ (L–M)	17e	−13.51	π (L)	$4b_1$	−14.56	π (phen)
									$15b_2$	−13.73	σ (L–M)	$3b_1$	−15.64	d_{xy}
												$14b_2$	−16.01	σ (L–M)
												17e	−16.04	$d_{xz,yz}$

[a] HOMO and LUMO are separated by the gap.
[b] The symbols used are π (L) for the π orbital localized along O–N–O linkage, π (phen) for the π orbital on the phenyl rings.

two groups in both the bonding and antibonding molecular orbitals which indicates that the M–L π interaction is highly covalent. For the late transition element Co, the energy levels of the d_π orbitals (free ion) and the ligand π orbitals (free ligand) are essentially the same, which leads to an intervening pattern of the metal based and ligand based molecular orbitals and a diminished HOMO–LUMO gap. For Ni, the energy levels of d_π orbitals (free ion) are significantly below those of the ligand π orbitals (free ligand) and the d_π–π interactions become minimal. The metal–ligand interactions in the Ni complex are thus limited to the σ type, and are of a more covalent character than any of the other complexes discussed here.

4. Discussion

4.1. Charge distributions

Since there are no occupied valence MOs with dominant metal d character in the Ti complex, Ti is in its highest oxidation state, 4+, and both HDBQI ligands are dianionic (Cat–N–SQ), which is consistent with the previous assignment [5]. Similarly, the absence of any occupied d orbitals and a large HOMO–LUMO gap leads to an unambiguous conclusion that V is also in its highest oxidation state, 5+. Therefore this complex should be assigned as V(Cat–N–SQ)(Cat–N–Cat) instead of $V(Cat–N–SQ)_2$ as suggested in an earlier report [5]. In addition, this assignment for the V complex fits the observed spectroscopic features better. The absence of the hyperfine structure due to ^{51}V in the EPR spectra is easily understood since the radical orbital (19e) is essentially ligand based. Furthermore, the formal reduction of one of the ligands to the Cat–N–Cat form should significantly raise the energy levels of ligand π orbitals and red-shift the LMCT in UV–Vis spectrum. This shift is responsible for the dissimilarity between the electronic spectra of the V complex and those of the complexes with two Cat–N–SQ ligands (Ge, Sn and Ti) [5].

The oxidation state of Mn was assigned as 4+ based on the relatively short Mn–N and Mn–O bond lengths [2]. Our calculation also points to a d^3 configuration, i.e. $d^2_{xz,yz}d^1_{xy}$, for the Mn center. The assignment of d^1_{xy} is unambiguous since the singly occupied HOMO has 61% d_{xy} character. While there is no orbital with more than 50% contribution from $d_{xz,yz}$, there are three orbitals containing significant $d_{xz,yz}$ character: 19e (35%), 18e (4%) and 17e (22%). This is best rationalized as that after the partial charge transfer ($2e^-$) the $d_{xz,yz}$ orbitals and the radical orbitals ($5b_2$) of the free ligands form unpolarized π type covalent bonds with the electron

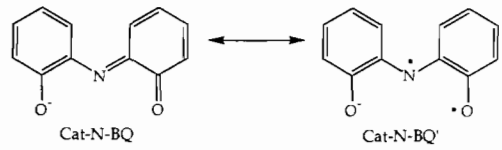

Scheme 2.

density evenly shared. In Ref. [2], this was interpreted as strong antiferromagnetic coupling between $d^2_{xy,yz}$ and the radicals localized on the ligands.

The Co complex was previously described as Co^{III}(Cat–N–SQ)(Cat–N–BQ) with $S=1/2$ due to a ligand centered radical [2]. The calculation clearly supports this description of a fully occupied t_{2g} set. In comparison with the Mn case, the energies of the d orbitals are lower and substantially below the $5b_2$ orbital of the free ligand. Hence the ligand is only capable of accepting three electrons from the e_g^* orbitals. The nature of the singly occupied HOMO being localized along the O–N–O linkage confirms the earlier assessment of the ligand centered spin density.

There is no doubt that the t_{2g} set in the Ni complex is fully occupied. However, the calculation seems to indicate that the $5b_2$ orbital of the free ligand is still well below the e_g^* set, which should enable complete transfer of four valence electrons from the e_g^* to the $5b_2$. Based on this description the complex should be designated as $Ni(Cat–N–SQ)_2$ with Ni in the 4+ oxidation state. Upon examining the characters of several low lying valence molecular orbitals, we found that both e_g^* orbitals also contribute significantly to two L–M σ bonding orbitals: $14b_2$ ($d_{x^2-y^2}$ 23%) and $14a_1$ (d_{z^2} 22%), although the contributions are smaller than those in the antibonding counterparts ($16b_2$ and $16a_1$). Therefore the e_g^* set, after partial electron transfer ($2e^-$), forms two unpolarized covalent M–L σ bonds with the σ orbitals from both N and O atoms. The complex is thus tentatively assigned as $Ni^{II}(Cat–N–BQ')_2$, where the biradical Cat–N–BQ′ is an alternative canonical form of Cat–N–BQ, as described in Scheme 2. One of the radicals in Cat–N–BQ′ is likely involved in the M–L σ bonding and the other corresponds to the unpaired electron in the 20e orbital.

4.2. Redox properties

Since the identities of the frontier orbitals for all the complexes have been unambiguously assigned, the discussion of the reversible redox processes is relatively straightforward. Four one-electron redox steps were observed for both Ti and Ni complexes, whereas MO analysis indicates that the HOMO is a pair of half-filled ligand π orbitals. Thus, in accord with the early analysis [3,5], the two oxidation steps correspond to the sequential removal of the first and second electrons from the HOMO, while the reductions are the addition

of electrons to the HOMO. Therefore all the redox steps occur at the ligands and the species involved in each step are summarized in the following equation:

$$M(SQ\text{–}N\text{–}BQ)_2 \underset{I}{\overset{e^-}{\rightleftharpoons}} M(Cat\text{–}N\text{–}BQ)(SQ\text{–}N\text{–}BQ) \underset{II}{\overset{e^-}{\rightleftharpoons}}$$

$$M(Cat\text{–}N\text{–}BQ)_2 \underset{III}{\overset{e^-}{\rightleftharpoons}} M(Cat\text{–}N\text{–}BQ)(Cat\text{–}N\text{–}SQ) \underset{IV}{\overset{e^-}{\rightleftharpoons}}$$

$$M(Cat\text{–}N\text{–}SQ)_2 \underset{V}{\overset{e^-}{\rightleftharpoons}} M(Cat\text{–}N\text{–}SQ)(Cat\text{–}N\text{–}Cat) \underset{VI}{\overset{e^-}{\rightleftharpoons}}$$

$$M(Cat\text{–}N\text{–}Cat)_2 \quad (1)$$

where the first four steps are applicable to the Ni complex and the last four to the Ti complex.

The neutral vanadium complex is assigned as V(Cat–N–SQ)(Cat–N–Cat). The removal and addition of an electron to the triply occupied HOMO 19e correspond to the only observed reversible oxidation (step V in Eq. (1)) and the low potential (−350 mV) reduction (step VI), respectively. Further oxidation (steps IV and III in Eq. (1)) is inhibited due to the build-up of positive charge at the V center. The third redox step corresponds to the addition of the second electron to the LUMO (20e, $d_{xz,yz}$) of the neutral complex. This step should require a significant potential difference due to the sizable HOMO–LUMO gap, and is indeed reflected by the voltammetry measurement, where the potential difference between the −1/−2 and 0/−1 steps is −1400 mV for the V complex and only −470 mV for the Ti complex.

The reversible oxidation of the Mn complex was attributed to the ligand [2], i.e. one of the Cat–N–SQ being oxidized to Cat–N–BQ. It appears that the oxidation is instead metal-centered, i.e. the removal of the d_{xy} electron, since (i) the d_{xy} is the singly occupied HOMO for the neutral complex, and (ii) the HOMO–SHOMO (SHOMO is the second highest occupied MO) gap is relatively large (~2.5 eV). As pointed out by Larsen and Pierpont [2], the two reductions are indeed metal based, since the LUMO is also a metal based orbital (20e, $d_{xz,yz}$). The species generated are Mn^{III} ($d^2_{xz,yz}d^2_{xy}$) and Mn^{II} ($d^3_{xz,yz}d^2_{xy}$).

MO analysis of the redox processes that occur in the Co complex is consistent with the earlier assignment [2]. Since the HOMO is the singly occupied ligand π orbital $5b_1$, the only oxidation is ligand based and corresponds to the removal of the electron from this orbital to generate the monocation complex $[Co(Cat\text{–}N\text{–}BQ)_2]^+$. The first reduction is naturally the addition of one electron to the HOMO, which leads to the formation of $[Co(Cat\text{–}N\text{–}SQ)_2]^-$. Since the LUMO is the metal $d_{x^2-y^2}$ orbital, the second reduction is metal based which generates a Co^{II} species.

4.3. Magnetic properties

The ferromagnetic coupling observed for $M^{IV}(CatN\text{–}SQ)_2$ (M as Ti, Sn and Ge) was attributed to a superexchange mechanism where a pair of mutually orthogonal empty metal orbitals mediate the coupling [5,12]. MO analysis for the Ti complex strongly supports this notion. The molecular orbitals representing the coupled organic radical are the 19e, which contain 7% $d_{xz,yz}$ character. The potential exchange between d_{xz} and d_{yz} will stabilize the triplet over the singlet by $2K$ (K is the exchange integral) multiplied by the $d_{xz,yz}$ contribution to the MO. Given the fact that K is approximately 10^3 cm^{-1} for a 3d metal, the coupling constant J would be ~ -70 cm^{-1}, which is close to that (-56 cm^{-1}) determined from the magnetic susceptibility measurements.

Although the magnetic properties of the neutral V complex are straightforward, it is interesting that the cationic species could be generated. According to the single-electron MO scheme derived from Fenske–Hall calculations, removal of one electron would generate $[V^V(Cat\text{–}N\text{–}SQ)_2]^{2+}$. Due to the largely increased $d_{xz,yz}$ contribution (17%) to the π-radical orbitals, a ferromagnetic coupling much stronger than that observed for the Ti complex is predicted.

5. Conclusions

The key to the understanding of the electronic structures of $M(HDBQI)_2$ is the position of the d_π (t_{2g} set) orbitals relative in energy to the ligand π orbitals localized along the O–N–O linkage (π(L)). Fenske–Hall calculations reveal that for the early transition elements Ti and V, d_π is much higher in energy, which enables a complete transfer of the metal valence electrons to the π(L)s. For the middle transition element Mn, a partial M–L charge transfer is preferred due to the close distribution of the d_π and π(L) orbitals in energy, and the M–L π interaction is more covalent. The late transition elements Co and Ni possess low energy d_π orbitals in which valence electrons are completely retained upon the formation of the complex. For the Ni complex, the degree of transfer of the e_g^* electrons cannot be resolved at the Fenske–Hall level and will be the subject of further magnetic and theoretical (SCF-Xα) studies.

6. Supplementary material

The full tabulations of the valence molecular orbitals calculated for both the free ligand CAT–N–SQ and all the above-mentioned metal complexes (Tables S1–S6) are available from the author upon request.

Acknowledgements

The author is grateful to the Florida Institute of Technology for financial support and Professor M.B. Hall for making the Fenske–Hall program available.

References

[1] A.Y. Girgis and A.L. Balch, *Inorg. Chem.*, *14* (1975) 2724.
[2] S.K. Larsen and C.G. Pierpont, *J. Am. Chem. Soc.*, *110* (1988) 1827.
[3] C.L. Simpson, S.R. Boone and C.G. Pierpont, *Inorg. Chem.*, *28* (1989) 4379.
[4] A. Caneschi, A. Dei and D. Gatteschi, *J. Chem. Soc., Chem. Commun.*, (1992) 630.
[5] S. Bruni, A. Caneschi, F. Cariati, C. Delfs, A. Dei and D. Gatteschi, *J. Am. Chem. Soc.*, *116* (1994) 1388.
[6] M.B. Hall and R.F. Fenske, *Inorg. Chem.*, *11* (1972) 768.
[7] D.J. Gordon and R.F. Fenske, *Inorg. Chem.*, *21* (1982) 2907.
[8] F. Herman and S. Skillman, *Atomic Structure Calculations*, Prentice-Hall, Englewood Cliffs, NJ, 1963.
[9] B.E. Bursten and R.F. Fenske, *J. Chem. Phys.*, *67* (1977) 3138.
[10] B.E. Bursten, J.R. Jensen and R.F. Fenske, *J. Chem. Phys.*, *68* (1978) 3320.
[11] F.A. Cotton, *Chemical Applications of Group Theory*, Wiley, New York, 3rd edn., 1990.
[12] O. Kahn, *Molecular Magnetism*, VCH, New York, 1993.